A. Folch
Center for Engineering in Medicine and
Surgical Services,
Massachusetts General Hospital,
Harvard Medical School,
Shriners Burns Hospital,
Boston, MA 02139

A. Ayon
Microsystems Technology Laboratories,
Massachusetts Institute of Technology,
Cambridge, MA 02139

O. Hurtado
Center for Engineering in Medicine and
Surgical Services,
Massachusetts General Hospital,
Harvard Medical School,
Shriners Burns Hospital,
Boston, MA 02139

M. A. Schmidt
Microsystems Technology Laboratories,
Massachusetts Institute of Technology,
Cambridge, MA 02139

M. Toner
Center for Engineering in Medicine and
Surgical Services,
Massachusetts General Hospital,
Harvard Medical School,
Shriners Burns Hospital,
Boston, MA 02139

Molding of Deep Polydimethylsiloxane Microstructures for Microfluidics and Biological Applications

Here we demonstrate the microfabrication of deep (>25 μm) polymeric microstructures created by replica-molding polydimethylsiloxane (PDMS) from microfabricated Si substrates. The use of PDMS structures in microfluidics and biological applications is discussed. We investigated the feasibility of two methods for the microfabrication of the Si molds: deep plasma etch of silicon-on-insulator (SOI) wafers and photolithographic patterning of a spin-coated photoplastic layer. Although the SOI wafers can be patterned at higher resolution, we found that the inexpensive photoplastic yields similar replication fidelity. The latter is mostly limited by the mechanical stability of the replicated PDMS structures. As an example, we demonstrate the selective delivery of different cell suspensions to specific locations of a tissue culture substrate resulting in micropatterns of attached cells.

Introduction

The handling and delivery of small quantities of liquid is a critical part of many physical, chemical, and biological processes, both in the laboratory and in Nature. Artificial microchannels (μChs) have served to run chemical microreactors (Srinivasan et al., 1997), to perform capillary electrophoresis assays (Woolley and Mathies, 1994), to probe red blood cell rigidity (Brody et al., 1995), and to transport living cells (Li and Harrison, 1997), among other uses. Generally, these μChs are fabricated by directly micromachining silicon (Si) or amorphous silicon oxide (glass) (Ristic, 1994). The crystalline structure of Si is particularly convenient because a KOH wet etch results in well-defined sidewalls (Petersen, 1982). After micromachining the three-dimensional profile of the μCh, the structure is sealed by high-temperature wafer bonding. This microfabrication method, albeit simple, has several disadvantages: (1) Wafer bonding is not compatible with the presence of heat-sensitive materials (such as a biomolecular layer or pattern) on either wafer at the time of bonding; (2) a single dust speckle on either wafer causes bonding to fail catastrophically; (3) after bonding, the μChs cannot be reused nor inspected because bonding is irreversible, which makes troubleshooting and analysis difficult; and (4) silicon must be excluded when a transparent substrate (e.g., for phase-contrast micros-

copy) is needed. Usually, Si may be substituted by glass (amorphous SiO_2) or, at an impractical cost, by quartz (crystalline SiO_2). The substitution of Si for glass faces additional problems: (1) Glass is not sensitive to most plasma-based (anisotropic) etches, hence etching vertical sidewalls in glass is tediously slow (typically, 100 times slower than Si); and (2) due to the amorphous nature of glass, a wet etch is necessarily isotropic and results in poorly defined geometries and/or severe, often uneven undercut of the layer used to mask the etch.

Organic polymers offer an attractive solution to the problems outlined above: There exists a variety of transparent polymers that can be replica-molded from another surface (the "master"). Considering that microlithography is only needed to fabricate the master, routine access to a sophisticated, expensive clean room facility is not necessary. The use of micromolded polymeric replicas in biology and medicine is not new. In 1986, Brunette created epoxy replicas of 0.5–2-μm-deep micromachined Si grooves to study contact-guidance of cells by microtopographic features on the substrate. Kapur et al. (1996) have cast and injection-molded biomedical polymers such as polydimethylsiloxane (PDMS), low-density polyethylene, poly-L-lactide, and polyglycolide with a replication fidelity of 90–95 percent from Si substrates containing features up to 8.5 μm deep. Electrophoretic separations of DNA have been achieved in injection-molded (McCormick et al., 1997) or imprinted (Martynova et al., 1997) plastic μChs. Recently, elastomeric μChs have been used as microfluidic templates to micropattern polymers (Kim et al., 1995), proteins (Delamarche et al., 1997), and cells (Folch and Toner, 1998).

From a microfluidics point of view, shallow μChs inevitably result in large pressure drops and large shear stresses (Potter and Foss, 1982) requiring strong sealing, high injection pressures, and/or low flow rates. However, for biological applications where live cells are injected into and/or attached inside the μChs (e.g., a microfabricated bioreactor, etc.), simulation of near-to-*in-vivo* conditions mandates that shear stress and concentration of nutrients, metabolic products, and oxygen be as close as possible to physiological levels. Similar constraints apply to cell separation assays and to the selective delivery of cell suspensions to particular locations of the substrate. A technology that allows for the fabrication of deeper μChs will enable designs that yield smaller pressure drops, improved mass transport, and/or larger perfusable areas. Others have utilized costly X-ray sources to pattern high-aspect-ratio structures of polymethylmethacrylate (500–2000 μm deep) (Guckel et al., 1996) or slow, serial three-dimensional laser micromachining to create Si microstructures (Bloomstein and Ehrlich, 1992; Mullenborn et al., 1995). Here we report our investigation on replica-molding of PDMS as an alternative to micromachined glass for microfluidics and cell culture applications, where a transparent substrate is indispensable. We have explored the feasibility of two candidate technological solutions for creating masters containing deep flat-bottom trenches. In both cases, a layered substrate is constructed such that the mold features can be carved on the top layer without attacking the bottom layer. Therefore, the height of the microstructures is dictated only by the initial bilayer construction and not by the pattern definition step. Different mask designs and layer thicknesses were used for each technological solution. General advantages and disadvantages of using either technology are discussed in the text, and cellular micropatterning by direct selective delivery of cell suspensions is demonstrated.

Materials and Methods

Silicon-on-Insulator (SOI) Wafers. SOI wafers, courtesy of Motorola, Inc., consisted of a "sandwich" of 37-μm-thick Si(100) layer atop a 1-μm-thick SiO_2 layer on a 500-μm-thick Si(100) wafer.

Photolithography of SOI Wafers. Standard photolithography was used to create a photoresist pattern of lines of different widths on the SOI wafers. To optimize photoresist adhesion, the SOI wafers were exposed to high-temperature vapors of hexamethyldisilazane (HMDS) prior to photoresist coating. Subsequently, they were spin-coated at 3000 rpm with 6.5 μm of the UV-sensitive photoresist AZ4620 (Hoechst Celanese Co., Sunnyvale, CA), baked for 30 min at 90°C, exposed to UV light (power 6 mW/cm^2, wavelength 320 nm) for 300 s through a chrome contact mask (Advance Reproductions, North Andover, MA) with a Karl Süss aligner, developed for 5 min in AZ440 developer (Hoechst Celanese Co.), and post-baked for 30 min at 90°C. The photoresist pattern was used to mask the plasma etch of the SOI wafers.

Deep Plasma Etch of SOI Wafers. The photoresist pattern was transferred to the 37-μm-thick Si layer in an inductively coupled plasma etcher (Surface Technology Systems, Palo Alto, CA) using time-multiplexed deep etching (Ayon et al., 1998). With this approach, the substrate is exposed for 15 s to a fluorine-rich plasma flowing only SF_6 (flow rate = 140 sccm, pressure = 24 mTorr, coil power = 600 W, substrate bias power = 12 W), and then the system is switched to a fluorocarbon-rich plasma flowing only C_4F_8 (flow rate = 95 sccm, pressure = 18 mTorr, coil power = 600 W, substrate bias power = 0 W) for 11 s, which coats all surfaces with a protective teflon-like film. To prevent plasma extinction during the gas switching operation, C_4F_8 flow is turned on 0.5 s before SF_6 flow is turned off, and vice versa. In the subsequent etching cycle, the expo-

sure to ion bombardment clears the polymer preferentially from horizontal surfaces and the cycle is repeated.

Fluorocarbon Layer Coating of Plasma-Etched SOI Masters. Before retrieving the wafers from the etcher, the wafers were coated with a 0.5-μm-thick fluorocarbon layer by exposure to a mixture plasma of C_4F_8 for 5 min. This teflon-like layer prevented bonding of the PDMS during curing and facilitated its release from the mold, eliminating the need for additional processing after etching of the master such as gold coating (Folch and Schmidt, 1998; Folch and Toner, 1998) or passivation with a self-assembled monolayer of methyl-terminated silane (Delamarche et al., 1997).

Photolithography of SU8-Coated Wafers. We used the commercially available EPON-SU8 (Microlithography Chemical Co. (MCC), Newton, MA) in one of either two formulations, SU8-50 or SU8-25, corresponding to viscosities that, according to the manufacturer's specifications, yield 50-μm- or 25-μm-thick films, respectively, when spun at 2500 rpm. In all cases, a quantity equivalent to a ~3-cm-radius area was dispensed in static conditions, allowed to spread for 15 s at 500 rpm, spun for 20 s at 750 rpm, baked for 25 min at 95°C on a horizontal hot plate, and exposed for 25 s with 325-nm-wavelength collimated UV light. This procedure resulted in ~50 μm and ~100 μm for SU8-25 and SU8-50, respectively. Precaution was taken to level the hot plate; unlike most photoresists, which harden at high temperatures, SU8 softens as temperature increases and flows toward the lowest part of the wafer if the wafer is slightly inclined. A Dektak profilometer was used to measure pattern height.

PDMS Replication. PDMS was prepared as a mixture of two liquid components (Sylgard 184 kit, Dow Corning). The curing procedure recommended by the manufacturer consists of mixing a PDMS precursor with a curing agent in a 10:1 ratio by weight, pouring the liquid mixture onto the Si mold, and waiting (~24 hours at room temperature, 6 hours at 60°C, or 1 hour at 150°C) until cured (Kumar and Whitesides, 1993; Kumar et al., 1994). The uncured mixture was first placed in a low vacuum (~20–30 Torr) powder-free dessicator (Nalgene) to evacuate the bubbles created during mixing. Breaking the vacuum periodically was necessary to pop the bubbles on the surface, which in turn allowed bubbles at lower depths to reach the surface. After pouring a ~5-mm-high layer of the mixture onto the masters, they were placed in low vacuum again to help evacuate the bubbles from narrow trenches. PDMS was overcured on the master molds for a length of time at least twice as long as that specified by the manufacturer, because slight undercuring has been shown to affect the release and stability of PDMS structures (Delamarche et al., 1997). Typically, PDMS was cured overnight at 40–60°C. For consistency, the replicas were carefully peeled off always in the direction parallel to the trenches; release in the direction perpendicular to the trenches resulted in a qualitatively lower replication yield for the smaller trenches (see below).

SEM Imaging. SU8 and PDMS samples were sputter-coated with a thin layer of Au/Pd prior to imaging to avoid charge buildup during imaging. The three-dimensional structure of these samples was best visualized by imaging at a 45 deg tilt angle and in dynamic focus mode to ensure proper focus over the whole image area.

Cellular Micropatterning. A ~100-μm-thick SU8 layer was exposed through a mask depicting a set of 200-μm-wide addressable lines with 200 μm spacing. The mask was made from imagesetting film and printed with a Hercules printer (Lino-type, Heidelberg, Germany) at 3386 dots per inch (~7.5 μm dot size) (Pageworks, Cambridge, MA). A PDMS replica was then cast as described above, with the following modifications. To enable fluidic access to the μChs, a post made of ~1-
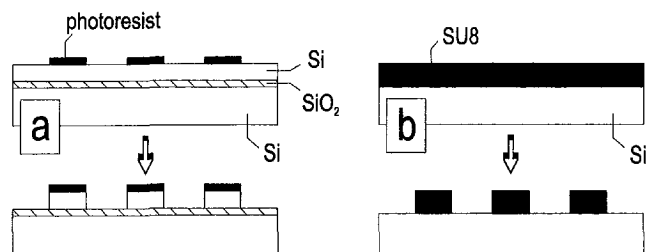
Fig. 1 Cross-sectional schematics of microfabrication process based on (a) anisotropic plasma etch of a photoresist-patterned silicon-on-insulator wafer, or (b) photolithographic patterning of SU8-coated wafer

mm-dia plastic tubing was glued with Duco cement (Devcon, Wood Dale, IL) at the inlet pad of each channel before pouring the PDMS precursor. Note that the post height ($\sim$1 cm) must be greater than the depth of the PDMS layer ($\sim$5 mm). After PDMS curing, with the plastic post still half-embedded into the PDMS layer, a piece of silicone tubing with an inner diameter smaller than the outer diameter of the first post was tight-fit onto it, and a second layer of PDMS precursor was poured. After complete curing of both PDMS layers, they were separated from the silicon wafer and the plastic post was pushed out of the PDMS-embedded silicone tubing. Since PDMS binds to the outer walls of the silicone tubing, this ensures a perfect sealing at the inlet. The μChs were then laid onto tissue culture-grade plastic dishes (Corning) and sterilized by overnight UV light exposure. Prior to injection, 3T3-J2 fibroblasts were incubated in CellTracker Green CMFDA or CellTracker Orange CMTMR (Molecular Probes, Eugene, OR) for 45 min at 37°C, trypsinized, and resuspended at a density of $\sim$5 million cells/mL, as measured with a hemecytometer. The cell suspension was introduced in a 3 cc syringe and slowly injected by hand into the μChs by inserting the syringe tip into the silicone tubing. The cells were allowed to attach for 2 hours before removing the μChs.

Results and Discussion

For microfluidics applications, it is critical to achieve optimum sealing between the PDMS μChs and the closing substrate of choice. We term "sealing surface" the surface of the PDMS μChs that contacts the closing substrate. Thus, since the μChs are replica-molded, the sealing surface corresponds to the *bottom* of the features in the master. Clearly, the features cannot be created by means of a timed plasma or wet etch because these etches result in a rough, tapered bottom and, most importantly, a width-dependent depth; a molded replica of such a master has a rough, poor sealing surface (data not shown) and only the features replicated from the deepest trenches actually contact the substrate. We have investigated two technological approaches for microfabricating deep flat-bottom trenches. Both approaches are based on a bilayered substrate: The chemistry used to pattern the top layer does not affect the bottom layer and, consequently, it does not determine the pattern height as long as the bottom layer is reached. These two approaches, schematized in Fig. 1, are: (1) a photoresist-masked plasma-etch of a Si layer bonded to a SiO$_2$ etch stop layer (Fig. 1(a)); and (2) direct photopatterning of thick photoresist layers made from "Nano-SU8" (heretofore referred to simply as SU8) a commercially available photosensitized epoxy (Fig. 1(b)).

Micropatterning of SOI Wafers. To test the resolution of master fabrication and replication fidelity, a set of trenches of various widths ranging 2–60 μm were etched for 40 min, as shown in the cross-sectional scanning electron microscopy (SEM) images of Fig. 2. The narrowest trench (2 μm wide) failed to reach the buried oxide layer by $\sim$3 μm (Fig. 2(a)); we attribute the slower etch rate in narrow trenches to scattering

of downward-accelerated ions by the trench walls and to diffusion-limited ion transport at large depth-to-width ratios. The scattering hypothesis explains also why the trench in Fig. 2(a) widens with increasing depth. It should be observed that the sidewall ripples visible in all the images in Fig. 2 reflect the periodicity of the etching chemistry cycles (see Materials and Methods); this cyclic procedure preserves the high etching rate of fluorinated chemistries but permits the etching of highly anisotropic profiles. However, there is an inherent scalloping produced in the walls due to the isotropic nature of the etch, which is also replicated in the molding operation (see below). The smoothing of the ripples (and its frequency increase) with increasing depth, clearly discernible in images $(a)-(e)$, is consistent with a diffusion-limited ion etch at large depth-to-width ratios effectively collapsing the cycles into a slower, more uniform etch. Note, also, that in images (b) and (c) the bottom of the trenches has suffered a re-entrant etch. This "footing" effect has been reported and explained by charge buildup in the oxide layer effectively deflecting impinging ions horizontally (Hwang and Giapis, 1997); one may also imagine a purely chemical scenario, where the reactive species that reach the inert oxide layer diffuse laterally to react with the Si walls. This would account for why the effect is only observed in high depth-to-width ratio trenches, where ion transport at large depths becomes diffusion-limited.

PDMS Replicas of SOI Masters. SEM images of the PDMS replicas of trenches of three different sizes corresponding to the trenches in Fig. 2(b, c, d) are depicted in Fig. 3(a) (top and bottom), 3(b) (top and bottom) and 3(c), respectively. There are several noticeable features. In general, the narrowest trenches of Fig. 2(a) were not replicated at all because the PDMS structures were torn during peel-off, with PDMS staying inside the trenches (data not shown). Trenches 5–10 μm wide (Figs. 2(b, c)), on the other hand, were faithfully replicated as demonstrated in Fig. 3(a, b), respectively. This is strongly surprising, given the large footing effect and sidewall ripples observed in Fig. 2(b, c). In some cases, the replica of the foot is torn off, as confirmed by the presence of a long hanging streak in Fig. 3(b) (top). We believe that the overall release yield can only be explained by the unusually large elasticity of PDMS. The 5-μm-wide PDMS structures, due to their high aspect ratio of $\sim$7.5, are unstable and prone to collapse sideways; almost all of the 5-μm-wide structures were sticking to their own PDMS base at some point along their whole length ($\sim$3 cm), as shown in Fig. 3(a) (bottom). This collapse was not observed on any of the 10-μm-wide structures (aspect ratio of $\sim$3.8) along their whole length. Overall, the replication of PDMS structures 20 μm wide (aspect ratio of $\sim$2) or wider was flawless. We stress that the images in Fig. 3 contain information on the three-dimensional profile of the trenches, which cannot be obtained from the SEM images of the masters (see Fig. 2); in particular, the plane of the sidewall has a wavy profile that is accentuated toward the end of the structure, possibly induced by asymmetries in the plasma field at the four-wall end of the trench. This is unlikely to be an artifact of the replication process or a plastic deformation during peel-off, since other features such as the foot and the sidewall ripple appear to be qualitatively undistorted. Even though a deep plasma etch allows for high-resolution patterning of large aspect ratio silicon structures, such large aspect ratios ($>$4), as shown above, are not stable when replicated in PDMS. Below we present a purely photochemical process as an alternative for the replication of mechanically stable PDMS structures with flat sealing surfaces.

Micropatterning of SU8-Coated Wafers. We have previously observed that PDMS binds moderately to glass and, by extension, to the native SiO$_2$ on Si (Folch and Schmidt, 1998). To avoid even partial bonding, which hinders release, the wafers were precoated with 1500 Å of Si$_3$N$_4$ in a standard LPCVD

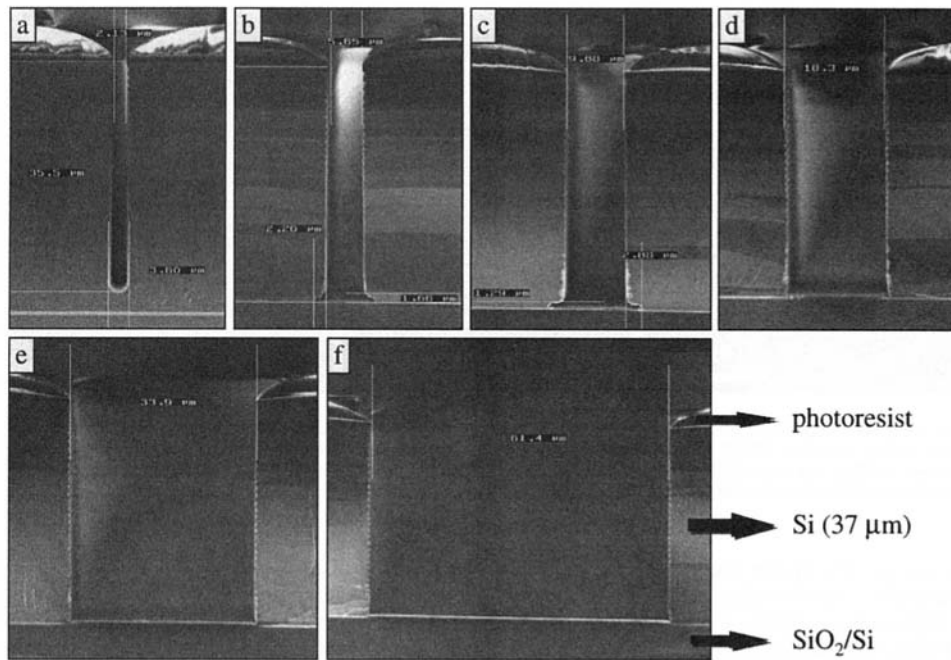## Deep plasma etch of SOI wafer

Fig. 2 Cross-sectional SEM images of plasma-etched microgrooves on a silicon-on-insulator wafer. Except for (a), all grooves have the same depth $D = 37$ μm as defined by the thickness of the initial silicon layer bonded onto SiO_2. Since the SiO_2 layer is not sensitive to the silicon-etching chemistry, the etch virtually stops at the Si-SiO_2 interface to produce flat-bottomed grooves. The cursor labels denote the width of the groove at the top (W_t) or at the bottom (W_b) portion of the groove, and the foot width (W_f) or height (H_f). (a) $D = 35.5$ μm, $W_t = 2.13$ μm, $W_b = 3.60$ μm; (b) $D = 37$ μm, $W_t = 5.65$ μm, $W_f = 2.26$ μm, $H_f = 1.66$ μm; (c) $D = 37$ μm, $W_t = 9.88$ μm, $W_f = 2.88$ μm, $H_f = 1.29$ μm; (d) $D = 37$ μm, $W_t = 18.3$ μm; (e) $D = 37$ μm, $W_t = 33.9$ μm; and (f) $D = 37$ μm, $W_t = 61.4$ μm.

furnace or, alternatively, with ~1000 Å of gold in an e-beam evaporator. SU8 is a relatively recent type of photoresist that allows for >100-μm-thick uniform layers and is compatible with conventional UV-exposure equipment. SU8 is based on a photosensitized epoxy resin or "photoplastic" disolved in gamma-butirylactone and a proprietary photo-acid generator,

Fig. 3 SEM images of the PDMS replica of the sample in Fig. 2, corresponding to trenches (a) 5 μm wide (see Fig. 2(b)), (b) 10 μm wide (see Fig. 2(c)), (a) 20 μm wide (see Fig. 2(d)); the bottom images in (a) and (b), displaying a different portion of the same trench as the image directly above them, are shown to illustrate the stability of the PDMS structure.

which generates hydrofluoric acid upon UV exposure. The photogenerated acid is harmless because it reacts instantaneously with the epoxy groups. This reaction cleaves the epoxy groups and creates a cross-linked polyether network, which is insoluble in the developer solution. Hence it is a negative photoresist. SU8 is sold in various concentrations, which determine its final thickness for a given spin speed (usually 2500 rpm), e.g., when spun at 2500 rpm, "SU8-50" results in a 50-μm-thick layer, "SU8-25" in a 25-μm-thick layer, "SU8-10" in a 10-μm-thick layer, etc. However, and probably due to SU8's high viscosity, the coated thicknesses vary widely depending on the exact coating procedure, including total amount dispensed, spinning time, ramping speeds, surface composition, baking time and/or temperature, specially for low spinning speeds. The influence of these parameters on standard photoresists is, by comparison, negligible. We found that SU8, in contrast with standard photoresists, is very insensitive to overdevelopment; for our range of thicknesses and exposures, the exposed wafers could be safely left in the developing bath for at least 10 min longer than what was necessary to develop the smallest features. A thorough characterization of SU8 has been presented elsewhere (Lee et al., 1995; Lorenz et al., 1997). We consistently used the same procedure (see Materials and Methods) and verified its reliability. It should be noted that a ~2-mm-wide edge bead forms on the edge of the wafer as a result of the surface tension of the coating; the edge bead, which can protrude over the wafer surface by as much as 10 percent of the total layer thickness (MCC, private communication), prevents the wafer from coming into hard contact with the mask during exposure. Ideally, projection or proximity photolithography should be used in combination with thick SU8 coatings. Layers of SU8 on Au-coated wafers processed under the same conditions as Si_3N_4-coated ones resulted invariably in smaller (~20 percent) thicknesses, proba-
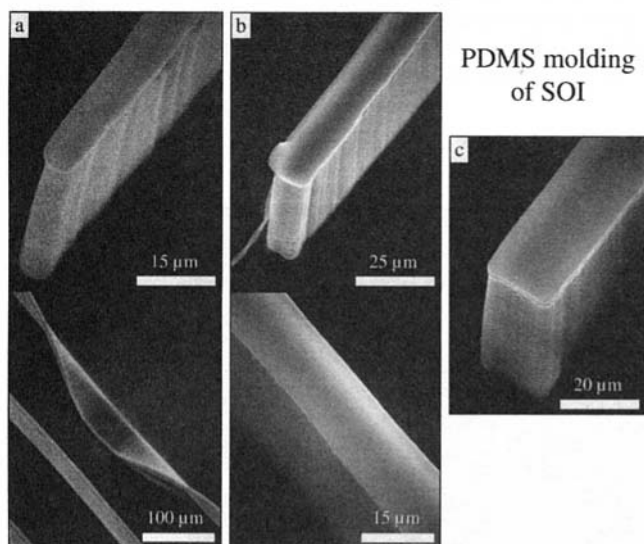
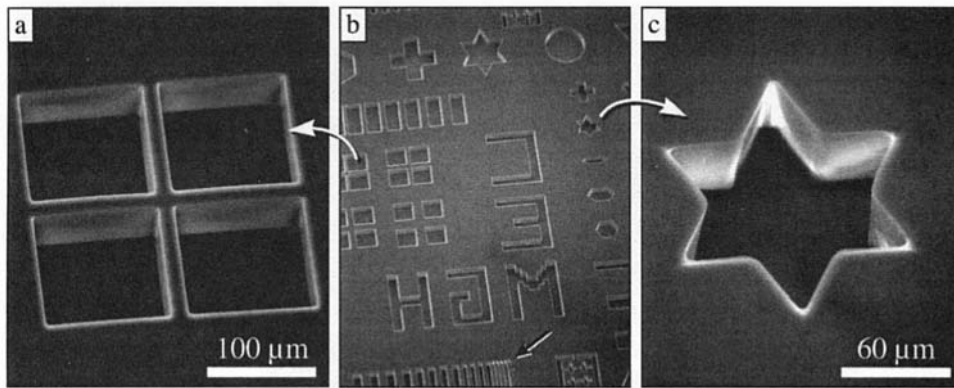## Photolithography of thick photoplastic SU8 layers

Fig. 4 SEM images of a photolithographically patterned 53-μm-thick SU8 layer on a Si_3N_4-coated Si wafer, after being used for PDMS replication. (a) and (c) display details of (b), as indicated by the large white arrows. In (b), the line width of the letters reading "CEM" in reverse is 50 μm. The straight black arrow points to a defect in the definition of the smallest features (see text).

bly due to gold's lower surface tension facilitating the centrifugal escape of liquid SU8 from the edge of the wafer during spinning. Figure 4 depicts three representative SEM images of 53-μm-high SU8 test structures created on Si_3N_4-coated wafers. The pictures were taken after molding and release of PDMS. In general, with the exception of the narrowest (5-μm-wide) trenches, which did not release the embedded PDMS (see Fig. 4(b)), white arrow), we did not observe signs of deterioration in the SU8 features after multiple PDMS replications, either by visual inspection, optical microscopy, or SEM imaging. Note that the lines in Fig. 4(a) are 10 μm wide (aspect ratio ~5). We stress that the sharp corners preserved along the full wall height (see Fig. 4(a, c)) are not easily obtained with standard photolithography. Despite the difficulties encountered during SU8 coating, we could routinely obtain <15-μm-wide lines or trenches of >50 μm height. Given the absence of contact between the mask and the SU8 surface, the sidewall verticality and sharp edge definition achievable with SU8 is surprisingly high.

PDMS Replicas of SU8 Masters. SEM images of the PDMS replica of the same wafer as in Fig. 4 are shown in Fig. 5. Similarly to the SOI wafer, the narrowest (5 and 10-μm-wide) trenches (Fig. 5(b), long white arrow) are not successfully replicated; the 5-μm-wide lines (aspect ratio ~10) were

torn during release, and the 10-μm-wide (aspect ratio ~5) collapse after release due to their high aspect ratio. These numbers agree well with the maximum aspect ratios achievable in PDMS replicas of SOI masters (see above). Sometimes, for medium-size, intricate structures such as the one in Fig. 5(a) (white arrow) and 5(b) (short white arrow) containing 25-μm-wide segments, can deform or tear partially during release. This effect is pattern-dependent, as 20-μm-wide straight lines separated by 20 μm (bottom of Fig. 5(b)) are successfully replicated. Absolute replication resolution cannot be straightforwardly quantified because proximity effects are very important. For example, a narrow (10-μm-wide) isolated SU8 line such as shown in Fig. 4(a) is replicated as a trench with high fidelity in Fig. 5(b) (grey arrow), whereas the set of 10-μm-wide lines (10-μm separation) in Fig. 4(b) (black arrow) is either torn during replication or collapses after replication (Fig. 5(b), long white arrow). We conclude that PDMS trenches with aspect ratios of 5 or higher are easily achieved, whereas a line of the same aspect ratio is either not replicated or unstable. This amply meets the design requirements of PDMS μChs for microfluidics applications: Since the pressure drop in a perfused μCh is mostly determined by the its cross section's smaller dimension (Potter and Foss, 1982), height-to-width ratios larger than 2 or 3 are not needed. As a rule of thumb, we infer that an array of
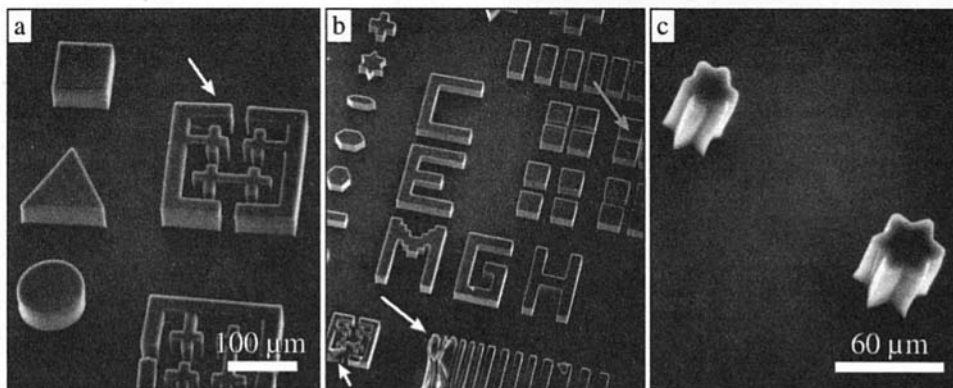
PDMS molding from SU8

Fig. 5 SEM images of the PDMS replica of the sample in Fig. 4. All three images display different regions of the sample. Note that (a) and (c) are displayed at high magnification. In (b), the line width of the letters reading "CEM" is 50 μm.
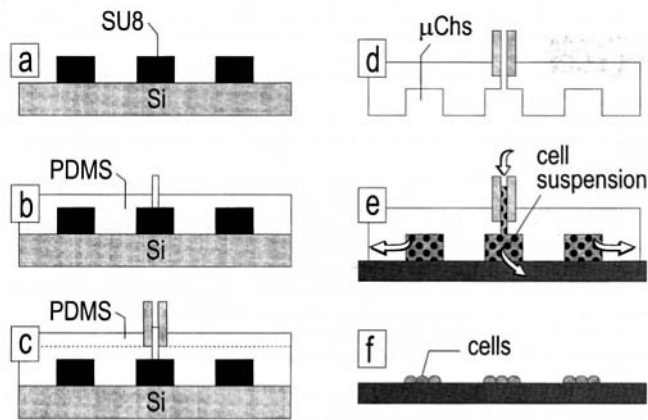
Fig. 6 Cross-sectional schematic of our cellular micropatterning method (see text for details). (a) SU8 micropattern on a silicon wafer; (b) casting of first PDMS layer (note the protruding plastic post); (c) casting of second PDMS layer (note the protruding silicone tube tight-fitted onto the plastic post); (d) PDMS microchannels (μChs) after separation from the Si wafer; (e) injection of cell suspension into the μChs; (f) cellular micropattern after removal of the μChs.

μChs (in parallel or networked configuration) could safely have, for optimum stability and sealing, a depth equal to the width of the narrowest channel and a minimum separation between channels equal to half that dimension. While the plasma etch of SOI wafers is comparatively far more expensive than SU8 photolithography, it is capable of higher resolution and may prove more suitable than SU8 for replication of other polymers by high-temperature injection molding, which requires a hard, high melting temperature mold substrate.

Applications of PDMS Microstructures in Biology. Among all biomedical polymers, PDMS stands out due to a unique property: It self-seals reversibly upon contact with a smooth dry surface, even in a non-clean room environment (Kim et al., 1995, 1996; Delamarche et al., 1997), probably because the elastomer establishes a highly conformal contact with the opposing surface. Hence, the (ambient temperature) sealing process is compatible with the presence of thin biochemical coatings, and both the PDMS structure and the closing surface can be analyzed after separation and reused (Delamarche et al., 1997; Folch and Toner, 1998). PDMS is biocompatible, implantable, and suitable for cell culture (Ratner et al., 1996). PDMS is an advantageous material for several additional reasons. PDMS, unlike other polymers that require injection-molding equipment (Kapur et al., 1996; Larsson et al., 1997), can be cast inexpensively at air pressure from a thermally curable mixture. The elastomeric nature of PDMS facilitates the release from the Si mold; after the PDMS replica is peeled off, the Si substrate remains intact and can be subsequently used several times to create other replicas. The replication fidelity is nanometric, as demonstrated by high-resolution microstamping of alkanethiols on Au surfaces with PDMS stamps (Kumar et al., 1994). Replication of vertical sidewalls, easily achievable on Si by plasma etch, is possible. Through-holes for backside access, not easily created in Si or glass, may straightforwardly be created at the time of molding from a glued standing post (Folch and Toner, 1998) (see below). The surface properties of PDMS, such as wetting or protein adhesion, may be tailored to some degree by oxygen-plasma oxidation (Morra et al., 1990) and/or by derivatization with self-assembled organosilane monolayers (Chaudhury and Whitesides, 1991, 1992; Chaudhury, 1993; Chaudhury and Owen, 1993). Its hardness can be adjusted within a certain range by varying the ratio of curing agent to PDMS precursor (Delamarche et al., 1997). We believe that these properties make PDMS an excellent candidate for microfluidics applications in biology, including cell rigidity and adhesion studies, cell transport in artificial capillaries, cell sorting, selective cell seeding on polymeric surfaces, and biosensors, to name a few.

Selective Delivery of a Cell Suspension. The process for creating a cellular micropattern is described in detail in Materials and Methods and schematized in Fig. 6. Briefly, our PDMS molding procedure consists of two steps. First, a small plastic post is glued to the inlet areas of an SU8 micropattern defining the μChs (Fig. 6(a)) and partially covered with PDMS precursor, which is allowed to cure (Fig. 6(b)). Second, a piece of silicone tubing is tight-fitted on the protruding post and partially covered with a second layer of PDMS precursor (Fig. 6(c)). PDMS binds to silicone but does not bind to the plastic post. As a result, when the cured PDMS is separated from the master, a tight seal between the silicone tubing and the PDMS is formed, whereas the plastic post can be easily pushed out (Fig. 6(d)). When the μChs are sealed against a suitable surface, a cell suspension can be selectively delivered to specific locations of the substrate (Fig. 6(e)). After cell attachment is complete and the μChs are removed, a cellular micropattern remains (Fig. 6(f)). As an example, we were able to create cellular micropatterns by directly injecting 3T3-J2 fibroblasts into μChs self-sealed against a tissue-culture dish. Cells were allowed to attach for 2 hours before removing the μChs. Separate cell suspensions could be injected into different μChs, as schematized in Fig. 7(a). Shown in Fig. 7(b) is a fluorescence + phase composite image depicting two 200-μm-wide lines formed of attached cells after removing the μChs. The green and red lines contain CellTracker Green-stained and CellTracker Orange-stained fi-
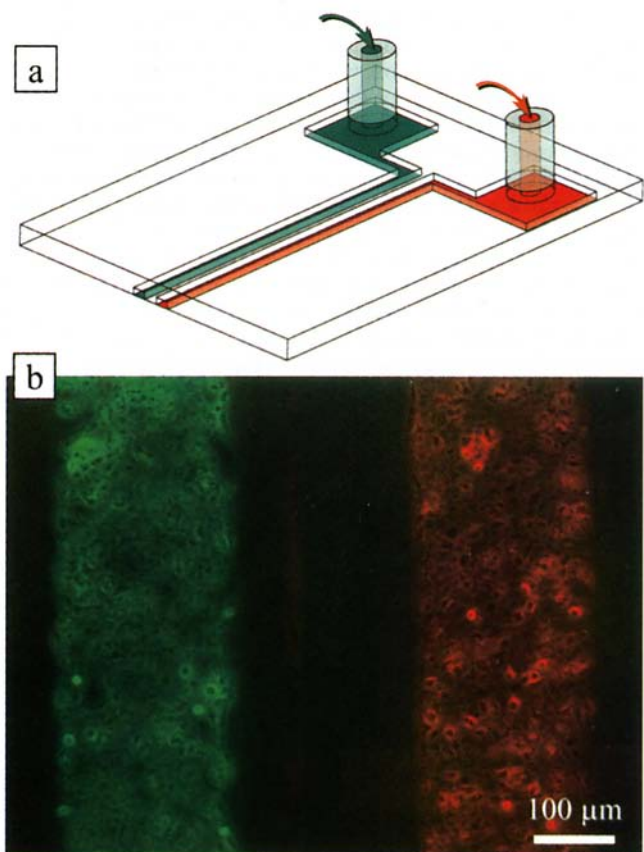

Fig. 7 (a) Three-dimensional schematic of the injection setup. The cell suspensions are introduced into the μChs at the vertical inlet areas as indicated by the arrows. Each color represents a different cell suspension. (b) Fluorescence + phase image of a micropattern containing red-stained and green-stained 3T3-J2 fibroblasts. Each line (200 μm-wide) was created by directly injecting a different cell suspension on adjacent, ~100-μm-deep μChs.

broblasts (see Materials and Methods), respectively. With this technique, one may straightforwardly create micropatterned co-cultures of two or more cell types on various materials, including homogeneous surfaces, and separated by a specifiable spacer. By contrast, previous techniques for creating micropatterned co-cultures required the creation of a template of differential adhesiveness prior to seeding by chemisorption (Bhatia et al., 1997) or physisorption (Folch and Toner, 1998) of protein patterns on a variety of surfaces; those methods required that one of the cell types adhered selectively to the protein patterns (a requirement that is incompatible with fibroblasts), only allowed for micropatterning at most two cell types, with each type necessarily attached to biochemically distinct surfaces and requiring contact between the two cell types. The method demonstrated here is not constricted by these requirements and could have many potential uses in studies of cell–cell interactions, biosensors, and tissue engineering.

Conclusions

We have been able to mold (i.e., cast *and* release) >50-μm-deep PDMS microstructures featuring flat sealing surfaces. We have successfully used two very dissimilar methods for the fabrication of the masters. A method using deep plasma etch of SOI wafers (patterned by standard photolithography) yielded very high resolution with slow, expensive processing, whereas a nonstandard photolithographic method using a thick photoplastic layer yielded satisfactory resolution with fast, inexpensive processing. These methods were compared only qualitatively, since the final goal—the replication of the masters in PDMS—is affected by many other parameters, such as master sidewall profile, release facilitation procedures, curing temperature, and/or curing chemistry, which were not optimized in this study. Without optimizing the aspect ratios achievable in the masters with either method, we *already* observe that the replication process is limited by the stability of the resulting PDMS structures. Therefore, we conclude that, for PDMS micromolding applications, accurate control of the master microfabrication process is not critical, as long as it guarantees that the resulting sealing surface will be flat. PDMS microstructures with non-flat sealing surfaces molded from plasma-etched plain Si wafers leak and detach from the surface in a matter of minutes; on the other hand, preliminary data shows that PDMS μChs molded from patterned bilayer wafers (be it SOI or SU8) stay sealed without observable leakage for at least three days (data not shown) when an aqueous solution is injected into them. As an application, we demonstrated the feasibility of micropatterning of more than two cell types without chemical modification of the surface. In this application, the narrowest line width achievable is limited by the mechanical stability of the microchannel walls (as explained above) as well as by the cell diameter in suspension. In addition, multicellular aggregates can partially obstruct the microchannel entrance and effectively dilute the microchannel-confined suspension. As a rule of thumb, a microchannel should be at least as deep and wide as the diameter of the cell in suspension.

Acknowledgments

References

Ayon, A. A., et al., 1998, "Etching characteristics and profile control in a time multiplexed inductively coupled plasma etcher," presented at the Solid State Sensor and Actuator Workshop, Hilton Head, SC.

Bhatia, S. N., M. L. Yarmush, and M. Toner, 1997, "Controlling cell interactions by micropatterning in co-cultures: hepatocytes and 3T3 fibroblasts," *J. Biomed. Mater. Res.*, 34(2): 189–199.

Bloomstein, T. M., and D. J. Ehrlich, 1992, "Stereo laser micromachining of silicon," *Appl. Phys. Lett.*, 61: 708.

Brody, J. P., Y. Han, R. H. Austin, and M. Bitensky, 1995, "Deformation and flow of red blood cells in a synthetic lattice: evidence for an active cytoskeleton," *Biophys. J.*, 68(6): 2224–2232.

Brunette, D. M., 1986, "Spreading and orientation of epithelial cells on grooved substrata," *Exp. Cell Res.*, 167(1): 203–217.

Chaudhury, M. K., and G. M. Whitesides, 1991, "Direct Measurement of Interfacial Interactions Between Semispherical Lenses and Flat Sheets of Poly(Dimethylsiloxane) and Their Chemical Derivatives," *Langmuir*, 7(5): 1013.

Chaudhury, M. K., and G. M. Whitesides, 1992, "Correlation Between Surface Free-Energy and Surface Constitution," *Science*, 255(5049): 1230.

Chaudhury, M. K., 1993, "Surface Free-Energies of Alkylsiloxane Monolayers Supported on Elastomeric Polydimethylsiloxanes," *J. Adhes. Sci. Technol.*, 7(6): 669.

Chaudhury, M. K., and M. J. Owen, 1993, "Correlation Between Adhesion Hysteresis and Phase State of Monolayer Films," *J. Phys. Chem.*, 97(21): 5722.

Delamarche, E., A. Bernard, H. Schmid, B. Michel, and H. Biebuyck, 1997, "Patterned delivery of immunoglobulins to surfaces using microfluidic networks," *Science*, 276(5313): 779–781.

Delamarche, E., H. Schmid, B. Michel, and H. Biebuyck, 1997, "Stability of molded polydimethylsiloxane microstructures," *Adv. Mater.*, 9(9): 741–746.

Folch, A., and M. A. Schmidt, 1998, "Wafer-level in-registry microstamping," *J. Microelectromech. Sys.*, in press.

Folch, A., and M. Toner, 1998, "Cellular micropatterns on biocompatible materials," *Biotechnol Prog.*, 14(3): 388–392.

Guckel, H., et al., 1996, "Advances in photoresist based processing tools for 3-dimensional precision and micro mechanics," presented at the Solid-State Sensor and Actuator Workshop, Hilton Head, SC.

Hwang, G. S., and K. P. Giapis, 1997, "On the origin of the notching effect during etching in uniform high density plasmas," *J. Vac. Sci. Technol. B*, 15(1): 70–87.

Kapur, R., B. J. Spargo, M. S. Chen, J. M. Calvert, and A. S. Rudolph, 1996, "Fabrication and selective surface modification of 3-dimensionally textured biomedical polymers from etched silicon substrates," *J. Biomed. Mater. Res.*, 33(4): 205–216.

Kim, E., Y. N. Xia, and G. M. Whitesides, 1995, "Polymer Microstructures Formed by Molding in Capillaries," *Nature*, 376(6541): 581.

Kim, E., Y. N. Xia, and G. M. Whitesides, 1996, "Micromolding in capillaries: Applications in materials science," *J. Amer. Chem. Soc.*, 118(24): 5722.

Kumar, A., H. A. Biebuyck, and G. M. Whitesides, 1994, "Patterning Self-Assembled Monolayers—Applications in Materials Science," *Langmuir*, 10(5): 1498.

Kumar, A., and G. M. Whitesides, 1993, "Features of Gold Having Micrometer to Centimeter Dimensions Can Be Formed Through a Combination of Stamping With an Elastomeric Stamp and an Alkanethiol Ink Followed by Chemical Etching," *Appl. Phys. Lett.*, 63(14): 2002.

Larsson, O., et al., 1997, "Silicon based replication technology of 3D-microstructures by conventional CD-injection molding techniques," presented at Transducers '97—International Conference on Solid-State Sensors and Actuators, Chicago, IEEE.

Lee, K. Y., et al., 1995, "Micromachining applications of a high resolution ultrathick photoresist," *J. Vac. Sci. Technol. B*, 13(6): 3012.

Li, P. C., and D. J. Harrison, 1997, "Transport, manipulation, and reaction of biological cells on-chip using electrokinetic effects," *Anal. Chem.*, 69(8): 1564–1568.

Lorenz, H., et al., 1997, "SU-8: a low-cost negative resist for MEMS," *J. Micromechanic. Microengineer.*, 7(3): 121.

Martynova, L., et al., 1997, "Fabrication of plastic microfluid channels by imprinting methods," *Anal. Chem.*, 69(23): 4783–9.

McCormick, R. M., R. J. Nelson, M. G. Alonso-Amigo, D. J. Benvegnu, and H. H. Hooper, 1997, "Microchannel electrophoretic separations of DNA in injection-molded plastic substrates," *Anal. Chem.*, 69(14): 2626–2630.

Morra, M., et al., 1990, "On the aging of oxygen plasma-treated polydimethylsiloxane surfaces," *Journal of Colloid and Interface Science*, 137(1): 11–24.

Mullenborn, M., H. Dirac, J. W. Petersen, and S. Bouwstra, 1995, "Fast 3D laser micromachining of silicon for micromechanical and microfluidic applications," presented at the 8th International Conference on Solid-State Sensors and Actuators, and Eurosensors IX, Stockolm, Sweden.

Petersen, K. E., 1982, "Silicon as a mechanical material," *Proc. IEEE*, 70(5): 420–457.

Potter, M. C., and J. F. Foss, 1982, *Fluid Mechanics*, Michigan, Great Lakes Press.

Ratner, B. D., A. S. Hoffman, F. J. Schoen, and J. E. Lemons, 1996, *Biomaterials Science: an Introduction to Materials in Medicine*, San Diego, Academic Press.

Ristic, L., ed., 1994, *Sensor Technology and Devices*, Boston, MA, Artech House.

Srinivasan, R., et al., 1997, "Micromachined reactors for catalytic partial oxidation reactions," *AIChE J.*, 43(11): 3059.

Woolley, A. T., and R. A. Mathies, 1994, "Ultra-high-speed DNA fragment separations using microfabricated capillary array electrophoresis chips," *Proc. Natl. Acad. Sci. USA*, 91(24): 11348–11352.